

# Enriching Multi-User OFDMA in Wi-Fi Networks with Frequency-Selective Channel Awareness

Kanghyun Lee, Youngwook Son, Jongyeon Park, and Saewoong Bahk

Department of Electrical and Computer Engineering and INMC, Seoul National University, Seoul, Republic of Korea

{khlee, ywson, jypark}@netlab.snu.ac.kr, sbahk@snu.ac.kr

**Abstract**—Recent studies on multi-user (MU) orthogonal frequency division multiple access (OFDMA) in IEEE 802.11ax highlight its advantages in terms of network efficiency under low traffic loads by mitigating channel access overheads. They also claim that MU-OFDMA becomes only susceptible to extra overheads under saturated traffic conditions, even leading to throughput loss compared to legacy single-user (SU) transmissions. Against this perspective, we notice that MU-OFDMA potentially enhances overall capacity of Wi-Fi networks by harnessing small resource units (RUs) flexibly over frequency-selective channels. Through measurements, we find that current RU allocation in commercial APs cannot achieve optimal performance due to the lack of consideration for detailed channel characteristics. We conceptualize a resource allocation strategy that accounts for distinct link quality across RUs, with its effectiveness verified through proof-of-concept study as well as extensive performance analysis. Based on these findings, we present *ChORUS*, a standard-compliant framework to realize optimal RU allocation by fully exploiting frequency-selective channels and their diversity among users. Our trace-driven simulation using standard channel models and real-world traces demonstrates that *ChORUS* significantly enhances throughput performance over SU, ensuring network capacity elevation through MU-OFDMA.

**Index Terms**—Wi-Fi, 802.11ax, multi-user OFDMA, resource allocation, frequency-selective channel fading.

## I. INTRODUCTION

IEEE 802.11 wireless local area network (WLAN), also known as Wi-Fi, has continually evolved to address pervasive performance challenges such as channel contention, increased latency, and unfairness, particularly arising in densely populated network environments. In pursuit of high efficiency (HE) Wi-Fi 6 (referring to its sixth generation), 802.11ax amendment incorporates many advanced features into its physical layer (PHY) specifications [1], aimed at enhancing network efficiency and user-experienced performance [2, 3].

One of the core technologies in 802.11ax is multi-user (MU) transmission based on orthogonal frequency division multiple access (OFDMA). This feature marks a fundamental shift from traditional single-user (SU) orthogonal frequency division multiplexing (OFDM) in legacy Wi-Fi networks. Unlike the SU transmission, which dedicates the entire bandwidth to serving only a single user at a time, MU-OFDMA enables

This work was supported in part by Institute of Information & Communications Technology Planning & Evaluation (IITP) grant funded by the Korea government (MSIT) (No. IITP-2025-RS-2024-00398157, IITP-2025-RS-2024-00429088) and in part by Samsung Electronics Co., Ltd (IO210208-08399-01).

Youngwook Son and Saewoong Bahk are the corresponding authors.

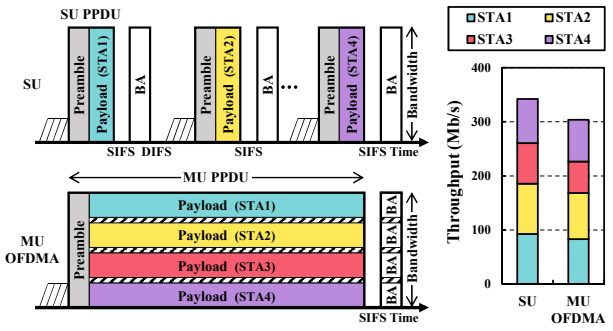


Fig. 1. Comparison of SU and MU-OFDMA transmissions with our preliminary measurement result.

simultaneous transmissions to/from multiple users by dividing the channel into smaller sub-channels, known as resource units (RUs). As illustrated in Fig. 1, an access point (AP) can allocate these RUs to different user stations (STAs)<sup>1</sup> in an MU-OFDMA transmission, with each RU being individually modulated in constructing MU PHY protocol data unit (PPDU).

Basically, MU-OFDMA amortizes transmission overheads i.e., random backoff, PHY preamble, and acknowledgement (ACK), across multiple users served at once, thus improving network efficiency. In this regard, numerous studies have highlighted that MU-OFDMA offers great advantages over SU under low traffic loads, by transmitting small-sized frames simultaneously to multiple users and thereby reducing user-perceived latency [4]. At the same time, those studies have doubted the effectiveness of MU-OFDMA from the network capacity perspective. They claimed that some extra overheads associated with MU may incur severe inefficiency, sometimes even resulting in performance loss compared to SU [5].

In this paper, we present a different point of view regarding the performance of MU-OFDMA in Wi-Fi networks. We start from a simple measurement in our testbed using commercial Wi-Fi devices, where AP enables either SU or MU-OFDMA transmissions to 4 associated users (STA1–STA4) under saturated traffic demands in downlink direction. The result is shown in Fig. 1 on the right; with MU-OFDMA, overall network throughput even reduces to lower than SU, which aligns with the findings in [5–8] as cross-validated through their simulation, theoretical analysis, and real measurements, respectively. However, from the preliminary measurement, we

<sup>1</sup>Throughout this paper, we use the terms “STA” and “user” interchangeably to denote a user station or device associated with Wi-Fi networks of interest.

further observe that RU allocation of the AP remains mostly unchanged despite different testbed setups including varied user locations. This implies that each user is served through the same RU fixedly among all possible sub-channel resources.

This observation has motivated us to question whether MU-OFDMA truly leads only to degradation in network capacity. To find the answer, we notice a different aspect of MU-OFDMA, that is, its ability to harness frequency resources of narrower bandwidth more flexibly. This gives crucial implications particularly in that Wi-Fi supports increasingly wider bandwidth, up to 160 MHz in 802.11ax, where each user can experience distinct link quality across RUs within the channel, due to frequency-selective fading effects. In this context, another potential benefit of MU-OFDMA arises, in terms of overall capacity rather than medium access, from allocating “good” RUs to individual users based on their own channel characteristics. In other words, we can enhance not only per-link data rates but also overall capacity of Wi-Fi networks through MU-OFDMA, by fully exploiting frequency-selective channels and their diversity among individual users.

In this paper, we explore this potential of MU-OFDMA in elevating overall network capacity. We scrutinize RU allocation of practical Wi-Fi networks, and develop a conceptual strategy that incorporates frequency-selective link quality into MU-OFDMA given the channel information. The effectiveness of this strategy is verified through proof-of-concept studies using real channel traces, as well as link and system-level analysis for characterizing its achievable performance. Based on our concept and findings, we present *ChORUS*, a standard-compliant framework for MU-OFDMA, which implements the frequency-selective RU allocation with the aid of practical channel sounding protocol of 802.11ax. We evaluate its performance through comprehensive system-level simulation using both the standard channel models and real-world traces.

To the best of our knowledge, this is the first work that spotlights performance of MU-OFDMA with respect to network capacity enhancements. Against the previous works that have overlooked this potential advantage of leveraging frequency-selectivity and diversity of wireless channel by its nature, our *ChORUS* enriches MU-OFDMA such that it can provide superior performance over SU in general even under saturated traffic loads, demonstrating its effectiveness and practicality as not limited to specific network scenarios.

## II. BACKGROUND AND RELATED WORK

### A. Multi-User OFDMA in Wi-Fi Networks

MU-OFDMA enables simultaneous transmissions to/from multiple users by dividing the entire channel into smaller RUs. Fig. 2 shows different types of RUs within 80 MHz channel bandwidth, ranging from the smallest 26-tone RU to the full 996-tone as defined in [1], where each RU type is named after the number of active subcarriers contained.

The main purpose of MU-OFDMA is to amortize redundant protocol overheads per individual channel access across multiple users, improving network efficiency in densely populated

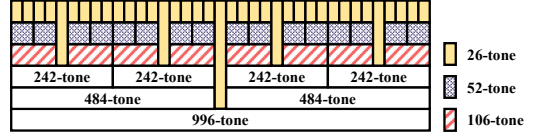


Fig. 2. Possible RU types in 80 MHz channel bandwidth.

environments [3]. Particularly, MU-OFDMA is highly beneficial under low or moderate traffic loads, as it allows AP to transmit small frames to its intended users at the same time and thus ensures much reduced latency [4, 9]. However, such latency reduction becomes marginal under heavy traffic loads, as bulky aggregate medium access control (MAC) protocol data units (A-MPDU) bring relatively minor overhead and rather lead to persistent delays in both SU and MU transmissions [8]. More importantly, for downlink traffic, extra overheads of MU transmissions, e.g., per-user signaling headers and ACK sequences, and wasted subcarrier tones, become more dominant and detrimental to overall efficiency.

Some previous studies have shown that average throughput of MU-OFDMA even reduces to lower than SU due to these extra overheads, cancelling out other benefits from MU transmissions, especially under saturated traffic conditions [5, 7]. In these contexts, most research efforts on MU-OFDMA have highlighted its benefits in terms of quality of service (QoS) under non-saturated traffic loads [6–8], or some have focused solely on uplink MU scenarios where the achievable network throughput could be boosted by virtue of increased transmit power density and reduced contention among STAs [5, 10]. But, regrettably, none of these prior work have explored another potential through MU-OFDMA by leveraging frequency-selective channels in practical environments.

### B. Resource Allocation and Frequency-Selective Fading

Detailed RU allocation for each MU transmission is not strictly specified by 802.11 standards, but is left to AP’s implementation-dependent algorithm. This flexibility allows different APs to employ varied strategies for MU-OFDMA, which can significantly impact overall network performance. In [10], AP allocates RUs to users as per estimated traffic characteristics, focusing on latency reduction through MU-OFDMA. Another framework in [11] treats RU allocation as a linear assignment problem, allowing AP to adapt utility function depending on different performance requirements. Similarly, throughput-maximizing scheduling was addressed in [12]. While this approach yields some improvements using specific modulation and coding schemes (MCSs), it sacrifices throughput of victim users thus leading to poor network fairness. Comprehensive studies on OFDMA in [5, 7] explored the impact of diverse network settings, e.g., different number of users, scheduling, and RU sizes. Their common observations indicate that allocating smaller RUs than the 242-tone is prone to throughput deterioration due to the extra MU overheads.

Meanwhile, frequency-selective channel fading poses another challenge in OFDM-based systems. Arising from multi-path signal propagation between transceivers, this fading effect may lead to poor channel quality encountered by specific subcarriers within an entire spectrum. Especially, increasingly

wider channel bandwidths in Wi-Fi—currently 160 MHz in 802.11ax, and 320 MHz in future standards [13]—have raised the chance of suffering “*deep fading*” at any segment of the channel [14]. This can result in a substantial loss in signal-to-noise ratio (SNR) over individual transmission links [15–17]. As for OFDMA RU allocation, most of existing approaches including the aforementioned ones have simply assumed flat fading conditions, not accounting for distinct channel quality across RUs and diversity among users. This oversight has led to under-estimation of network capacity achievable through MU-OFDMA, taking negative throughput gain over SU.

Only a few recent works on MU-OFDMA have addressed these channel characteristics. RU allocation framework in [18] adopts a greedy algorithm based on estimated channel state information (CSI). Focusing solely on uplink scenarios, however, this framework cannot exploit frequency-selective channels since all received frames at AP have equalized SNR levels.<sup>2</sup> The other approaches in [20, 21] employ a divide-and-conquer strategy or CSI prediction using deep neural networks respectively, both aiming at efficient RU allocation for combined MU multi-input and multi-output (MU-MIMO) and MU-OFDMA. While their performance was verified with respect to individual links for 20 MHz channel, the impact of extra MU overheads has not been accounted for by system-level evaluation, especially in comparison with SU in dense deployment scenarios [22]. Again, none of these studies noted the potential benefits of MU-OFDMA in leveraging frequency-selective fading and channel diversity. Although some prior researches on cellular and open-RAN have considered frequency-selective channel characteristics for energy efficiency [23, 24], they lack practicality and are not aligned with Wi-Fi standards. We elaborate in this paper on how this potential can be realized in its concept and practice, thereby elevating not only per-link performance but also overall capacity of Wi-Fi networks.

### III. MOTIVATION STUDY

We first conduct a motivation study based on real testbed measurements, to investigate how a commercial Wi-Fi AP manages MU-OFDMA transmissions including RU allocation in practical scenarios. Our primary goal is to examine whether the current implementations achieve optimal performance and, if not, to further identify potential enhancements.

#### A. Experimental Setup

For testbed setup, we employ a representative commercial AP, ASUS RT-AXE7800, equipped with Broadcom BCM6756 chipset supporting Wi-Fi 6 features based on 802.11ax. On user side, four Linux machines equipped with Intel AX210 network interface cards (NICs) serve as non-AP STA devices, ensuring the support of Wi-Fi 6 compatibly with the associated AP. While we deploy AP at a fixed location, each STA device is randomly placed at one of distributed locations in an office environment, as depicted in Fig. 3. Due to non-line-of-sight indirect signal paths with surrounding objects, this testbed

<sup>2</sup>For uplink MU procedure, AP requires transmit power control of participating STAs to adjust received signal strengths to the same target level [19].

Parameter	Value
Channel bandwidth	80 MHz
# spatial stream	1 (SISO only)
Rate control alg.	Enabled (default)
OFDMA RU	242-tone per STA
Traffic type	Downlink UDP (Saturated)
ACK sequence	Aggregated MU-BAR (no explicit BAR)

Fig. 3. AP & user deployment layout and experimental setup.

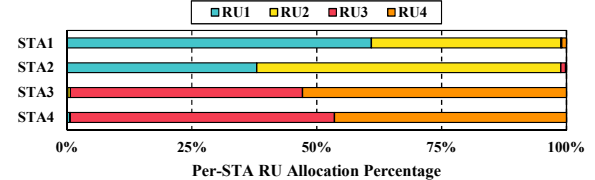


Fig. 3. AP & user deployment layout and experimental setup.

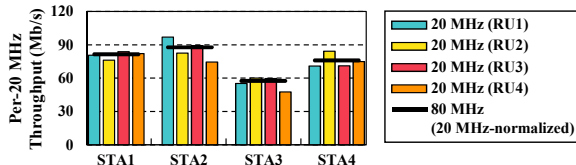
introduces a variety of frequency-selective fading effects on individual transmission links, reflecting typical indoor channel characteristics. We also strictly maintain stationary conditions during the measurements so as to minimize channel variations, interference, and any external influences.

#### B. Results and Observations

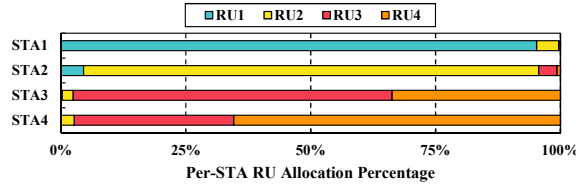
We configure AP operating in an 80 MHz channel to enable MU-OFDMA transmissions with four 242-tone RUs allocated to 4 STAs being simultaneously served. These RUs are indexed as RU1–RU4 in order, from the lowest to highest frequency band within 80 MHz. Other configurations are shown in Fig. 3, and follow baseline 802.11ax specifications unless noted otherwise. We conduct measurements across 20 different deployment scenarios each lasting 30 seconds, thereby capturing about 56,000 MU transmissions in total. Fig. 4 shows percentages of per-user RU allocation in MU-OFDMA transmissions over all our measurements, where the association ID (AID) of each STA remains unchanged as denoted by STA1–STA4. We observe that STA1 and STA2 are mostly served using RU1 and RU2 respectively, while RU3 and RU4 are allocated to STA3 and STA4. This pattern implies that the current RU allocation at AP is not entirely random or in an adaptive manner, in that the proportion of RUs neither follows a uniform distribution nor exhibits any dependence on varied deployment scenarios despite distinct channel conditions.

We further investigate how effectively each user is served under the current RU allocation regime. Taking one of selected deployment scenarios from Fig. 3 as an example, we configure AP to try SU transmissions instead of MU-OFDMA, using each of four 20 MHz sub-channels within the same 80 MHz as before. Indeed, these sub-channels correspond to the 242-tone RUs in MU-OFDMA, i.e., RU1–RU4. We compare per-20 MHz throughput of each STA between different RU locations as well as with that using full 80 MHz bandwidth (996-tone RU).<sup>3</sup> The measurement results are presented in Fig. 5(a), where the throughput of 80 MHz is given as a normalized

<sup>3</sup>We set AP's transmit power differently between 20 MHz and 80 MHz measurements to maintain the same power spectral density.



(a) Per-20 MHz single-user throughput compared between different RU locations (RU1–RU4) and full 80 MHz bandwidth (normalized)



(b) RU allocation percentages in actual MU-OFDMA transmissions

Fig. 5. Illustrative case study with a selected user deployment.

quantity by simply dividing the measured throughput by 4, for comparison with per-20 MHz performance.

In Fig. 5(a), per-20 MHz throughput of each STA varies with RU locations. Considering our interference-free testbed, such variation is only attributed to frequency-selective fading within the entire 80 MHz. More specifically, STA2 and STA4 achieve the highest throughput at RU1 and RU2 locations respectively, which outperform the normalized throughput of 80 MHz. This suggests that the effective use of separate RUs in OFDMA can provide more opportunity for individual users to enjoy better link quality by avoiding possible *deep fading* at certain segment of the entire channel. Disappointedly, actual OFDMA RU allocation in Fig. 5(b) for this specific deployment case does not align with throughput-maximizing STA–RU pairs from our observations. While the optimal combination can be found from the per-20 MHz measurements as {STA1–RU4, STA2–RU1, STA3–RU3, and STA4–RU2}, AP’s actual MU-OFDMA transmissions never follow this. We observe even some worst configurations being used for individual users, e.g., RU2 for STA1, RU4 for STA3, and RU3 for STA4. From this, we conclude that the currently inefficient RU allocation leads to under-utilization of network capacity, i.e., far from that optimally achievable through MU-OFDMA, due to the lack of consideration for distinct channel quality across RUs and among different users.

#### IV. BRINGING FREQUENCY-SELECTIVE CHANNELS INTO OFDMA RESOURCE ALLOCATION

As inferred from our previous observations, frequency-selective channels can play a crucial role in fully implementing the potential enhancements of MU-OFDMA. Without careful consideration of this, such an advanced OFDMA feature in modern Wi-Fi networks becomes only susceptible to severe inefficiency, even outperformed by legacy SU transmissions as revealed in Fig. 1. To bridge this gap, we present a conceptual methodology to accomplish optimal OFDMA resource allocation by exploiting distinct channel quality across RUs.

##### A. Proposed Concept of Frequency-Selective RU Allocation

To describe the underlying concept, we assume that AP has full knowledge of detailed channel quality for individual users,

on the per-subcarrier basis within an entire channel bandwidth. Our core strategy is to find optimal RU allocation based on the expectation of achievable data rates computed for every configurable STA–RU pair. To this end, we start with building an user-perceived performance metric which incorporates frequency-selective fading effects. Considering a general  $N \times N$  MIMO system with minimum mean-squared error (MMSE) receivers, we denote a perfect CSI matrix of the  $k$ -th subcarrier by  $\mathbf{H}_k \in \mathbb{C}^{N \times N}$ , for individual transmission link between AP and a specific STA. Then for the  $k$ -th subcarrier of the  $i$ -th spatial stream, post-processing SNR (PPSNR) [25] encountered by the receiving STA is given as<sup>4</sup>

$$\gamma_k^{(i)} = \frac{\rho^{(i)} \times |\{\mathbf{W}_k \mathbf{H}_k\}_{i,i}|^2}{\rho^{(i)} \times \sum_{s \neq i} |\{\mathbf{W}_k \mathbf{H}_k\}_{i,s}|^2 + |\{\mathbf{W}_k \mathbf{W}_k^H\}_{i,i}|^2}, \quad (1)$$

where  $\rho^{(i)}$  stands for nominal SNR value calculated as the ratio of mean received signal power of the  $i$ -th stream to the overall noise variance.  $\mathbf{W}_k \in \mathbb{C}^{N \times N}$  is the MMSE coefficient matrix that can be obtained from  $\mathbf{H}_k$  and  $\rho^{(i)}$  by

$$\mathbf{W}_k = [\mathbf{H}_k^H \mathbf{H}_k + (1/\rho^{(i)}) \mathbf{I}]^{-1} \mathbf{H}^H. \quad (2)$$

Using this PPSNR quantity for each subcarrier, we can derive effective SNR of available RU configurations following the same procedures as in [26, 27]. For any  $p$ -th OFDMA RU with its component subcarrier set denoted by  $\mathcal{K}_p$ , the effective SNR for an MCS index,  $m$ , can be obtained by

$$\text{eSNR}_p^{(m)} = \Phi_{(m)}^{-1} \left( \frac{1}{N \times |\mathcal{K}_p|} \sum_{i=1}^N \sum_{k \in \mathcal{K}_p} \Phi_{(m)}(\gamma_k^{(i)}) \right), \quad (3)$$

where  $\Phi_{(m)}(\cdot)$  denotes the received bit mutual information rate (RBIR) mapping function for a given MCS index  $m$ , and  $\Phi_{(m)}^{-1}$  is its inverse mapping [28].<sup>5</sup> Widely accepted as a key metric reflecting the impact of frequency-selective link quality including *deep fading*, this effective SNR yields an equivalent packet error rate (PER) under flat fading as with frequency-selective channels. Accordingly, the maximum data rate,  $\Lambda(p)$ , achievable through the  $p$ -th RU can be expected as

$$\Lambda(p) = \max_{m \in \mathcal{M}} \left[ \left\{ 1 - \Omega_{(m)}(\text{eSNR}_p^{(m)}) \right\} \times R(m) \right], \quad (4)$$

where  $\mathcal{M}$  is the supported MCS set, while  $R(m)$  and  $\Omega_{(m)}(\cdot)$  indicate specified PHY rate and typical SNR-to-PER mapping respectively, both for the MCS index  $m$  with  $N$  streams.

As the above procedure is carried out for individual link between AP and a specific STA, we can obtain this performance metric per every pair of STA and available RU by iterating (1)–(4). Letting  $\Lambda(p, q)$  denote the achievable rate expected by (4) for the  $p$ -th RU allocated to  $q$ -th STA, we suppose that AP schedules an MU-OFDMA transmission with the entire bandwidth comprising  $N_{\text{RU}}$  equal-sized RUs, and the number

<sup>4</sup>For notation,  $\{\cdot\}_{a,b}$  represents the  $(a,b)$ -th element of the matrix.

<sup>5</sup>RBIR mapping functions are typically implemented through pre-computed lookup tables, with ongoing parameter adjustments based on link statistics.

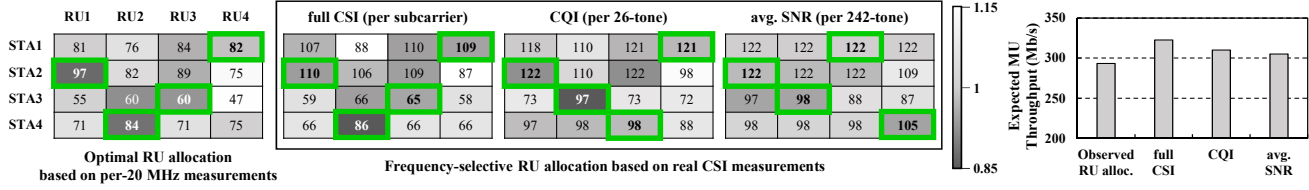


Fig. 6. Proof-of-concept for the case of Fig. 5: Throughput measurements vs. Frequency-selective RU allocation using real CSI traces.

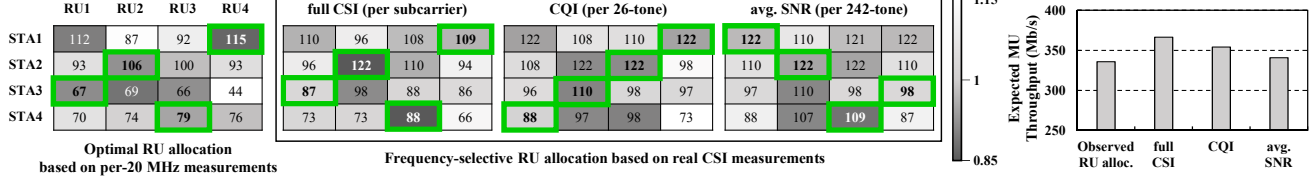


Fig. 7. Proof-of-concept for the case of Fig. 1: Throughput measurements vs. Frequency-selective RU allocation using real CSI traces.

of candidate users to be served is  $N_{STA}$ , equal to or more than  $N_{RU}$ . We can find the best RU allocation strategy to maximize aggregate data rate of a single MU-OFDMA transmission by solving the following optimization problem:

$$\begin{aligned} & \max_{\{x(p,q)\}} \sum_{p=1}^{N_{RU}} \sum_{q=1}^{N_{STA}} x(p,q) \Lambda(p,q) \\ \text{subject to } & \sum_{p=1}^{N_{RU}} x(p,q) \leq 1, \quad \forall q \in [1, N_{STA}] \\ & \sum_{q=1}^{N_{STA}} x(p,q) \leq 1, \quad \forall p \in [1, N_{RU}] \end{aligned} \quad (5)$$

where  $x(p,q)$ 's are RU allocation indicators; set to 1 if  $p$ -th RU is allocated to  $q$ -th STA, or set to 0 otherwise.<sup>6</sup>

### B. Proof-of-Concept using Real Channel Traces

To validate our concept, we conduct proof-of-concept experiments using real-world channel traces. Indeed, we have collected all channel traces in each deployment scenario for the previous experiments in Section III, using the well-known CSI extraction tool, PicoScenes [30]. We apply the frequency-selective RU allocation strategy to these real channel traces, i.e., computing (1)–(4) based on each CSI set, and solving (5) to find optimal allocation of four 242-tone RUs (RU1–RU4) to STA1–STA4. By comparing the result with real measurements of per-20 MHz throughput across different RU locations, we can verify the accuracy and effectiveness of our strategy taking into account frequency-selective channel characteristics.

In Fig. 6, the leftmost colormap represents a 4-by-4 matrix whose elements mark per-20 MHz measured throughput for corresponding STA–RU pairs among total 16 allocation cases as in Fig. 5(a). Other three colormaps in the middle provide the results of our RU allocation strategy when applied to real channel traces in this scenario, according to three different types of available CSI—full (raw) CSI on per-subcarrier basis, channel quality indicator (CQI) and average SNR (avg. SNR) given per 26-tone or 242-tone RU respectively. In each of these colormap matrices, its own optimal combinations of STA–RU

<sup>6</sup>As this optimization problem is formulated as a linear assignment problem, it can be effectively solved using the Hungarian algorithm, as shown in [29].

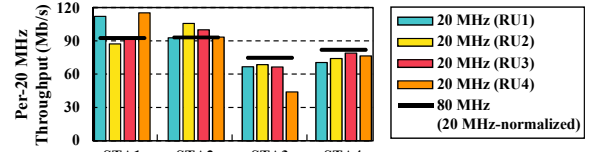


Fig. 8. Comparison of per-20 MHz user throughput between RU locations (RU1–RU4) and full 80 MHz bandwidth.

pairs are determined as those indicated with green boxes, either based on real measurements or upon the expected data rates using CSI. Comparing the resulting optimal combinations between the colormaps, we observe that our frequency-selective RU allocation using full CSI exactly matches with that from per-20 MHz measurements, while using CQI or avg. SNR leads to suboptimal results due to their inaccuracies in capturing frequency-selective channel quality with coarse granularity.

Getting back to Fig. 1, we can explain the inferior performance of MU-OFDMA. Without careful consideration for RU allocation as observed in Section III, each user is gaining no benefit of OFDMA and only suffers from extra overheads. However, per-20 MHz measurements on this case also reveal that individual users experience distinct link quality across RU1–RU4, as shown in Fig. 8. Hence, we can boost their throughput and thus the overall performance of MU-OFDMA by adopting more strategic RU allocation. Repeating the same proof-of-concept experiments, Fig. 7 presents the optimal combinations of STA–RU pairs in this scenario along with the agreement between our measurements and those derived using full CSI. In the rightmost of Fig. 6 and Fig. 7, we further compare expected MU-OFDMA throughput between the observed RU allocation and desired RU allocation (green boxes) found by our strategy using each type of CSI. These results confirm potential enhancements by exploiting frequency-selective channels in MU-OFDMA, over the currently inefficient RU allocation of commercial AP, while also demonstrating more optimized performance achievable through fine-grained CSI.

## V. CHARACTERIZING MU-OFDMA PERFORMANCE

### A. Multi-User Diversity and Link Capacity

We explore optimal performance of MU-OFDMA with the frequency-selective RU allocation presented in Section IV,

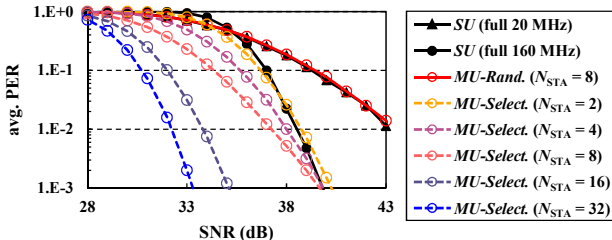


Fig. 9. Average PER performance (MCS 11) under frequency-selective channels, compared between SU and MU-OFDMA.

given the ideal CSI of all users. To assess per-link capacity enhancements, we employ MATLAB WLAN Toolbox [31], one of the most credible platforms for end-to-end system modeling and evaluation. Applying IEEE 802.11 channel models [32] for typical indoor scenarios, its end-to-end link-level simulation yields PER curves for each OFDMA RU configuration.

While our frequency-selective RU allocation aims to maximize aggregate data rates, given which MCS to be used for MU-OFDMA, the problem reduces to obtaining minimal PER for individual users with respect to per-link capacity. From this perspective, we compare average PER performance for the highest MCS 11 between SU and MU-OFDMA, according to different RU sizes, number of candidate users ( $N_{STA}$ ), and RU allocation policies, as shown in Fig. 9. The SU transmissions (SU with full 20 MHz or 160 MHz) harness the entire channel bandwidth in serving each single STA, while all MU-OFDMA transmissions (MU-Rand. and MU-Select.) are carried out with up to 8 simultaneous users, configuring equal-sized RUs of 242-tone (for  $N_{STA} \geq 8$ ), 484-tone (for  $N_{STA} = 4$ ), or 996-tone (for  $N_{STA} = 2$ ) within the same 160 MHz channel.

In Fig. 9, PER of SU with 160 MHz is far lower than that of 20 MHz, despite more chance of containing *deep fading* within the wider bandwidth. We attribute this to the error correction capability of LDPC for 160 MHz, which randomizes erroneous segment across more subcarrier tones than in 20 MHz. For MU-Rand. with  $N_{STA} = 8$ , eight 242-tone RUs are randomly allocated to 8 users with no consideration for distinct channel quality across different RU locations and individual users. As a result, average PER of MU-OFDMA with this policy is merely equivalent to that of SU with 20 MHz, failing to take advantage of the diverse channel characteristics.

On the contrary, for MU-Select. which adopts our frequency-selective RU allocation, the best STA-RU combinations are determined based on per-link achievable rates. This offers each user more opportunity to enjoy better link quality within its own RU instead of the full channel bandwidth. Accordingly, average PER of MU-Select. gets more reduced with larger  $N_{STA}$ , due to fine granularity with smaller RU sizes (up to  $N_{STA} = 8$ ) and diversity among users. Such enhancements in PER performance (equivalently, in SNR) indicate the elevation of overall link capacity for MU-OFDMA. Fig. 10 illustrates conceptually how the effective end-to-end link of an MU-OFDMA transmission is constructed by assembling preferable segments among the entire channels of all individual users.

Lastly, for  $N_{STA} \geq 8$ , average PER of MU-Select. keeps further enhanced by virtue of channel diversity among more

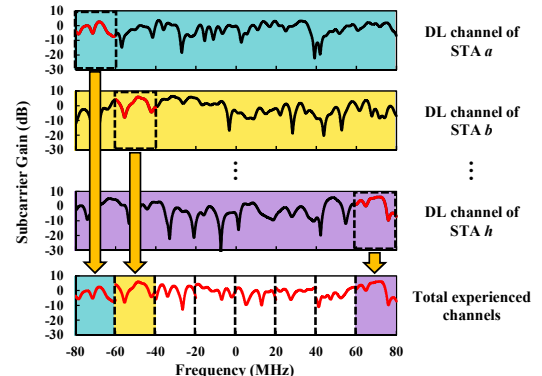
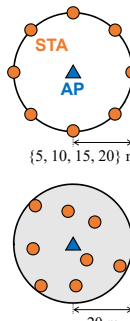


Fig. 10. Effective link capacity of an MU-OFDMA transmission with frequency-selective resource allocation.



Parameter	Value
Channel fading	TGax “D” NLOS / Real-world CSI traces
Channel bandwidth	160 MHz
# spatial stream	1 (SISO only)
Rate control alg.	Enabled (Minstrel)
OFDMA RU	242-tone per STA
Transmit power	20 dBm (AP) 15 dBm (STA)
Traffic type	Downlink UDP (Saturated)
ACK sequence	Aggregated MU-BAR (no explicit BAR)
A-MPDU size	Maximum (~ 5.4 ms)

Fig. 11. Simulation setup with FD/RD topology.

candidate users. However, we notice that realizing this benefit in actual OFDMA RU allocation would lead to the sacrifice of user fairness from the viewpoint of overall network. This is because our frequency-selective RU allocation policy only accounts for per-link capacity of a single MU-OFDMA transmission in principle, as will be addressed in Section VI.

### B. Overall Network Capacity Perspectives

Beyond the per-link capacity, we move on to potential enhancement in network performance by applying the frequency-selective resource allocation for MU-OFDMA. Identifying the effectiveness of our concept from this perspective is essential in that MU-OFDMA involves extra overheads incurring network inefficiency, particularly under saturated traffic loads.

**Methodology.** Due to the limited scalability of real testbeds, we employ ns-3 [33], the most popular system-level simulator, with the latest updates for 802.11ax features including MU-OFDMA. Prior to simulation run, we have refined Wi-Fi module of ns-3 to include the effects of frequency-selective channel fading, while the default implementation does not cover such a complex physical aspect due to its simplified PHY abstraction. In more detail, we have extracted the model-based channel traces from MATLAB WLAN Toolbox in the form of per-subcarrier fading gain along with its time-varying effects, following the similar methodology as used in [34]. Incorporating these traces to ns-3 with random realization, we have also modified receiver PHY model to reflect realistic performance under frequency-selective channels, referring to [25].

Our detailed simulation settings are shown in the table of Fig. 11, while we build a controlled network topology for

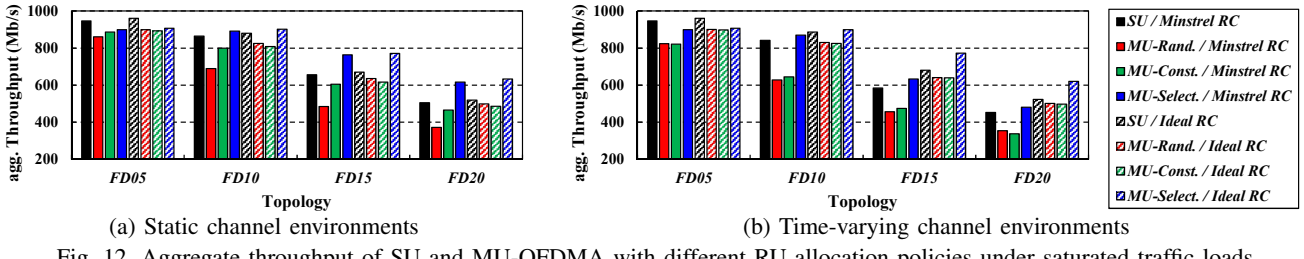


Fig. 12. Aggregate throughput of SU and MU-OFDMA with different RU allocation policies under saturated traffic loads.

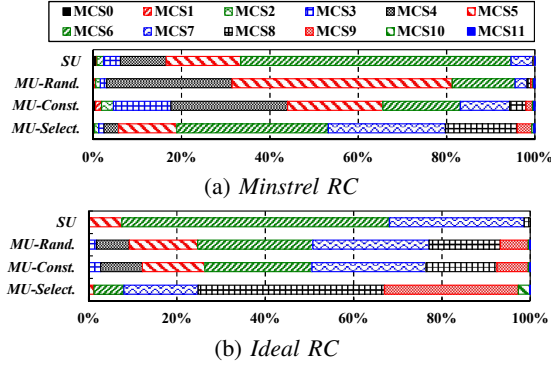


Fig. 13. Used MCS distribution in *FD20* under time-varying channel.

investigation. To be specific, AP and user deployment follows fixed distance topology (*FD*) as illustrated in the upper left of Fig. 11, consisting of a centered AP and 8 users located at a fixed distance from the AP. Similarly to the link-level simulation, we compare SU (*SU* with full 160 MHz) with MU-OFDMA under different RU allocation policies, i.e., AP allocates eight 242-tone RUs within 160 MHz to 8 users through random allocation (*MU-Rand.*) or with fixed STA–RU pairs (*MU-Const.*), or adopts our frequency-selective allocation (*MU-Select.*) assuming the ideal CSI available at AP.

**Simulation results.** Fig. 12(a) and (b) present aggregate network throughput under saturated traffic loads in static and time-varying channel environments, respectively. We compare the performance of *SU*, *MU-Rand.*, *MU-Const.*, and *MU-Select.*, each enabling either Minstrel rate control [35] (*Minstrel RC*) or ideal rate control (*Ideal RC*), with increasing distances between AP and users from 5 to 20 meters (*FD05*–*FD20*). For closer distances like *FD05*, most users enjoy extremely high SNR conditions due to negligible path loss, making every transmission carried out using the highest MCS. This explains relatively small difference between MU-OFDMA with different policies, as shown in *FD05* of Fig. 12(a), while their throughput loss compared to *SU* only comes from extra MU overheads. With this extreme link quality, *MU-Select.* cannot identify any potential enhancement because frequency-selective channel fading is left as a minor component in achievable data rate. As the distance increases up to *FD20*, *MU-Select.* achieves its intended performance gain over *SU* and other MU-OFDMA policies through the frequency-selective RU allocation, e.g.,  $\times 1.19$  throughput over *SU* and  $\times 1.24$  over *MU-Rand.* and *MU-Const.* with *Ideal RC*.

Meanwhile, we note the importance of OFDMA RU allocation with relation to rate control mechanism. In particular, allocating random RUs makes each user likely to encounter whole

different link condition in every MU-OFDMA transmission. This leads to its link statistics getting messed up by inconsistent transmission results, based on which the rate control does only malfunction or deteriorate as revealed by poor performance of *MU-Rand.* compared to *MU-Const.* in Fig. 12(a). Notably, this performance gap disappears in time-varying channels, where *MU-Rand.*, *MU-Const.* and even *MU-Select.* achieve far lower throughput using *Minstrel RC* than *Ideal RC*. It is because the heuristic mechanism fails to select the optimal MCS under channel variations. In such dynamic environments, *Minstrel RC* tends to conservatively use lower MCSs, as can be seen in Fig. 13, indicating under-utilization of channel resources.

On the whole, for any scenarios of varying distances, channel variation, and rate control methods, *MU-Select.* provides significant enhancements over *MU-Rand.* and *MU-Const.*, and even outperforms *SU* except for *FD05* topology, despite extra MU overheads. This verifies the effectiveness of our concept in elevating overall network capacity beyond the per-link data rates, by virtue of fully exploiting frequency-selective channel characteristics within MU-OFDMA transmissions.

## VI. PROPOSED FRAMEWORK: CHANNEL-AWARE MU-OFDMA RESOURCE ALLOCATION AND SCHEDULING

Motivated by the above challenges in handling frequency-selective channel characteristics and currently inefficient RU allocation, we present a comprehensive framework, named frequency-selective **C**hannel-aware MU-OFDMA **R**esource allocation and **U**ser **S**cheduling (*ChORUS*), which builds on the conceptual foundation in Section IV, specifically addressing three critical issues: Dependence on CSI, deterioration in rate control and user fairness, and the inefficient power assignment by AP at its maximum rate. The overview of *ChORUS* is illustrated in Fig. 14, presenting its integrated components.

### A. CSI Acquisition

The performance of channel-aware RU allocation is highly dependent on precise CSI acquisition at AP, essential for taking into account dynamic link conditions experienced by users. For *ChORUS*, we leverage the HE sounding protocol in 802.11ax to facilitate this CSI acquisition, involving several key steps: null data packet announcement (NDPA), NDP, beamforming report poll trigger frame (BFRP TF), and BFR, as depicted in Fig. 15. The sounding process begins with AP announcing an upcoming NDP transmission to target STAs through NDPA. After NDPA and NDP frames, AP sends out BFRP TF to solicit uplink MU transmissions, collecting BFRs from the target STAs.

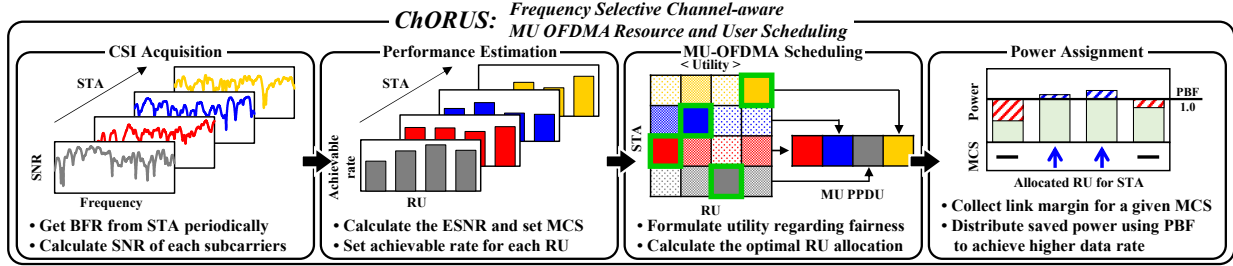


Fig. 14. Overview of the proposed framework, *ChORUS*, for MU-OFDMA transmissions with frequency-selective channel awareness.



Fig. 15. Sequence of HE sounding protocol within *ChORUS*.

To estimate the effective SNR for each RU, the HE MU exclusive beamforming report and the HE CQI report provide SNR data for individual subcarriers and the average SNR across subcarriers within each 26-tone RU, respectively. However, due to its limited SNR range, the HE MU exclusive beamforming report often results in an inaccurate estimation of effective SNR. Our evaluations suggest that using the CQI report and conducting the HE sounding protocol every 50 ms is an effective strategy. This approach provides a good balance between SNR accuracy and protocol overhead.

### B. RU Allocation and Rate Control

To incorporate the effects of frequency-selective channel environment into our approach, we use the RU allocation method formulated in Section IV, as outlined in Fig. 14 for performance estimation and MU-OFDMA scheduling. This method assesses each RU by calculating the achievable data rate and determines the RU allocation maximizing the total achievable data rate per transmission. While the method proves effective, it does not address fairness when there are more STAs than available RUs, nor does it incorporate rate control.

To address scenarios where the number of STAs exceeds the  $N_{RU}$ , we cycle through  $N_{RU}$  STAs among all available STAs in a rotating manner for each transmission and conduct RU allocation with these  $N_{RU}$  STAs. Although this method yields sub-optimal RU allocation for each individual transmission due to limited candidates, our analysis shows that having  $N_{RU}$  candidate users is sufficient to exploit the diversity of channel conditions effectively.

Regarding rate control, our analysis reveals that *Minstrel RC* has difficulty selecting proper MCS leading to a performance discrepancy between the *Minstrel RC* and the *Ideal RC*. To mitigate this gap, we retain the selected MCS,  $m$ , which aims to maximize the achievable data rate as defined in (4), during the calculation of RU allocation. Additionally, we introduce a link offset to buffer against inaccuracies, enhancing the robustness of the connection under fluctuating channel conditions. The link offset is set to 1 dB, accounting for the expected difference between the calculated and actual effective SNR at the receiver. This results in a more conservative selection of MCS, ensuring greater stability in data transmission.

### C. Power Assignment

In Wi-Fi networks, it is common for a STA to experience a gap between the required SNR for the selected MCS and the actual effective SNR, known as the link margin. This gap arises due to the discrete nature of MCS levels, and the required effective SNR for a given MCS can be determined by comparing the achievable data rate at different SNR levels.

The power boost factor (PBF), a feature in the 802.11ax standard, allows for varying power spectral density (PSD) levels across different RUs. This feature enables a direct multiplication of the signal amplitude by PBF ranging from 0.5 to 2, resulting in PSD gaps of up to 12 dB among RUs. Despite its potent capabilities, this feature is often underutilized until this work. This is largely because PBF alone does not significantly impact throughput performance when used solely.

Our strategy involves utilizing these link margins by reducing power to the required SNR for a given MCS and assigning the saved power to STAs that can achieve an elevated MCS with the smallest power increment—specifically, the gap between the required effective SNR of the current and the next higher MCS. This process includes iterative power assignment, where we continuously reassess and distribute the remaining power until there are no more STAs that can benefit from an MCS increment, or when the residual power is insufficient for further enhancements. Any remaining power after the process is distributed equally among the scheduled STAs. This power assignment mainly aims not to waste power as a link margin especially that of STAs close to AP, but to strategically assign to improve data rates across the network.

## VII. PERFORMANCE EVALUATION

### A. Based on IEEE 802.11 Channel Models

In this section, we employ the random distance topology (*RD20*) as depicted in Fig. 11, where STAs are randomly positioned within a 20 m radius for comprehensive evaluation. During the evaluation, we exponentially increase the number of STAs from 2 to 32, while keeping other simulation parameters consistent, as specified in Fig. 11. Differing from the comparisons in Section V-B, we substitute *MU-Select.* to *ChORUS* and introduce *MU-Greedy*, a scheme that heuristically adapts to channel fading and allocates RUs greedily, inspired by [18].

TABLE I: HoL delay in *RD20* (ms)

# STA	2	4	8	16	32
<i>SU</i>	11.08	22.37	44.37	89.38	178.52
<i>MU-Const.</i>	5.70	5.73	5.78	11.53	23.25
<i>MU-ChORUS</i>	5.72	5.72	5.72	11.45	22.93

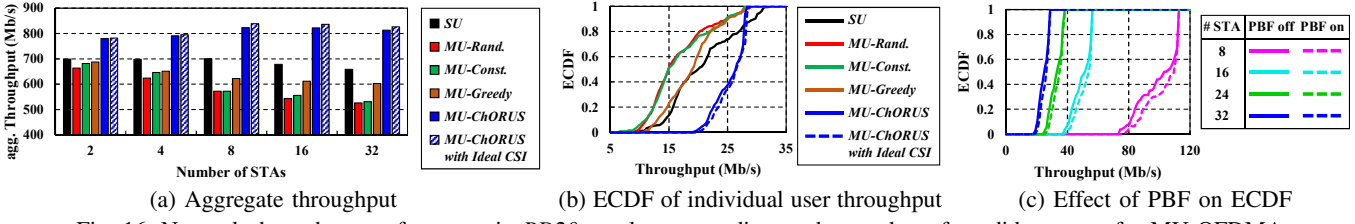


Fig. 16. Network throughput performance in *RD20* topology according to the number of candidate users for MU-OFDMA.

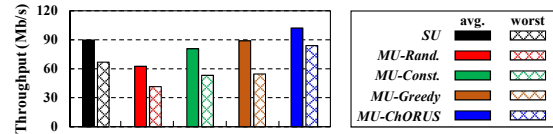


Fig. 17. Trace-driven evaluation result using real-world CSI.

*MU-ChORUS with Ideal CSI* operates without requiring the HE sounding protocol to obtain CSI at the STA, while *ChORUS* and *MU-Greedy* updates channel information only after the periodic reception of BFR. *Minstrel RC* is implemented for all schemes except *ChORUS*, which employs the previously described rate control approach. Consistent with the settings used previously, we use two 996-tone RUs and four 484-tone RUs for cases with two and four STAs, respectively. In all other cases, we choose the eight 242-tone RUs configuration.

As demonstrated in Fig. 16(a), *ChORUS* shows a significant improvement in throughput performance. Despite the overhead associated with MU transmission and the HE sounding protocol, *ChORUS* achieves significantly higher aggregate throughput, outperforming *SU* and *MU-Greedy* by 24% and 35% respectively, in the 32-STA case. Additionally, the performance of *ChORUS* closely matches that of *MU-ChORUS with Ideal CSI*, implying negligible loss from the CSI acquisition process. Unlike other schemes in comparison, *ChORUS* effectively exploits the channel diversity among users, and thereby maintains its performance even with a large number of STAs.

Fig. 16(b) presents the empirical cumulative distribution function (ECDF) of individual user throughput in the 32-STA case. Most STAs served by *MU-Rand.* and *MU-Const.* suffer from poor throughput due to inadequate RU allocation and rate control malfunctions under fading conditions. In contrast, a larger proportion of STAs with *ChORUS* can enjoy improved performance. Then the crossover between *ChORUS* and *SU* is attributed to extra MU overheads, which restrict achievable throughput of *ChORUS*. Fig. 16(c) further demonstrates the impact of power assignment via PBF on individual user throughput. Expectedly, the power assignment helps *ChORUS* better serve the users in relatively poor link conditions, even not affecting others with better performance.

Due to the simultaneous transmissions in MU-OFDMA, all *MU* schemes exhibit inherently reduced head-of-line (HoL) delays compared to *SU*, as shown in Table I. Remarkably, *ChORUS* also maintains low HoL delays, despite its additional overheads from the sounding process for CSI acquisition.

#### B. Trace-Driven Evaluation

To accurately simulate real-world channel characteristics into our evaluation, we record 40 trace files, each lasting

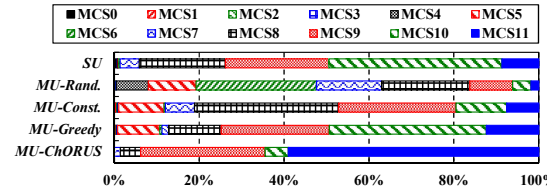


Fig. 18. Used MCS distribution in *RD20* under real channel traces.

15 seconds, across a 160 MHz bandwidth in a typical office setting. We then evaluate *ChORUS* in *RD20* with eight STAs.

As illustrated in Fig. 17, *ChORUS* continues to demonstrate superior performance, achieving higher average and worst throughput compared to other strategies. Notably, *MU-Const.* and *MU-Greedy* exhibit remarkably higher throughput than observed in previous tests using TGax channel model. The difference is attributed to the implemented real-world traced channels, which generally have slow and sporadic variance. This variance contrasts with the TGax channel, enabling *MU-Const.* and *MU-Greedy* to perform more consistently and effectively under steady conditions. Moreover, due to *ChORUS*'s rate control and power assignment strategies, there is a great improvement in MCS selection as shown in Fig. 18.

In summary, our proposed scheme, *ChORUS*, demonstrates significant performance enhancements under the *RD20* scenario with both the TGax channel model and real-world channels. This improvement is evident across various metrics, including maintaining consistent performance as the number of STAs increases and notably enhancing the throughput of all STAs. These results validate the effectiveness of *ChORUS* in resource allocation and adapting to diverse channel conditions, thereby enhancing overall network performance.

## VIII. CONCLUSION

This paper explored an efficient resource allocation method tailored for fading channel environments. We developed a channel-aware RU allocation method and validated its effectiveness using measured data. Through link- and system-level implementations, we identified practical challenges and introduced *ChORUS*, a refined scheme addressing key issues such as CSI acquisition, RU allocation, rate selection, and power assignment. Our approach leveraged frequency selectivity to enhance MU-OFDMA performance, as demonstrated in both modeled and real-world channel conditions. Comprehensive simulations demonstrated that *ChORUS* substantially improves network-wide throughput, fairness, and reduces latency, underscoring its effectiveness in adapting to complex channel dynamics and maintaining robust network performance.

## REFERENCES

- [1] IEEE 802.11ax-2021, *Part 11: Wireless LAN Medium Access Control (MAC) and Physical Layer (PHY) specifications. Amendment 1: Enhancements for High-Efficiency WLAN*, IEEE std., Feb. 2021.
- [2] B. Bellalta, "IEEE 802.11 ax: High-Efficiency WLANs," *IEEE Wireless Commun. Mag.*, vol. 23, no. 1, pp. 38–46, 2016.
- [3] D. J. Deng, Y. P. Lin, X. Yang, J. Zhu, Y. B. Li, J. Luo and K. C. Chen, "IEEE 802.11ax: Highly Efficient WLANs for Intelligent Information Infrastructures," *IEEE Commun. Mag.*, vol. 55, no. 12, pp. 52–59, Dec. 2017.
- [4] B. Li, Q. Qu, Z. Yan, and M. Yang, "Survey on OFDMA-Based MAC Protocols for the Next Generation WLAN," in *Proc. IEEE WCNC Workshops*, 2015.
- [5] S. Avallone, P. Imputato, G. Redietteab, C. Ghosh, and S. Roy, "Will OFDMA Improve the Performance of 802.11 WiFi Networks?" *IEEE Wireless Commun. Mag.*, vol. 28, no. 3, pp. 100–107, 2021.
- [6] H. Dev, U. Sikka, J. Kulshrestha, and M. Maity, "When Is Multiple Access Beneficial? An Analysis of Multi-User Performance in IEEE 802.11ax," in *Proc. ACM MobiWac*, 2022.
- [7] D. Magrin, S. Avallone, S. Roy, and M. Zorzi, "Performance Evaluation of 802.11ax OFDMA through Theoretical Analysis and Simulations," *IEEE Trans. Wireless Commun.*, vol. 22, no. 8, pp. 5070–5083, 2023.
- [8] R. Liu and N. Choi, "A First Look at Wi-Fi 6 in Action: Throughput, Latency, Energy Efficiency, and Security," in *Proc. ACM Meas. Anal. Comput. Syst.*, 2023.
- [9] S. Brahma, M. Yazid, and M. Omar, "Multiuser Access via OFDMA Technology in High Density IEEE 802.11ax WLANs: A Survey," in *Proc. IEEE EDiS*, 2020.
- [10] M. Inamullah, B. Raman, and N. Akhtar, "Will My Packet Reach on Time? Deadline-Based Uplink OFDMA Scheduling in 802.11ax WLANs," in *Proc. ACM MSWiM*, 2020.
- [11] S. Lin, H. Qi, X. Wen, Z. Lu, and Z. Hu, "An Efficient Group-Based OFDMA MAC Protocol for Multiuser Access in Dense WLAN Systems," in *Proc. IEEE ICC Workshops*, 2018.
- [12] M. S. Kuran, A. Dilmac, O. Topal, B. Yamansavascilar, S. Avallone, and T. Tugcu, "Throughput-Maximizing OFDMA Scheduler for IEEE 802.11ax Networks," in *Proc. IEEE PIMRC*, 2020.
- [13] IEEE 802.11be-2023, *IEEE Proposed TGbe draft specification, IEEE P802.11be/D5.0*, IEEE std., Nov. 2023.
- [14] J. Suh, Y. Yoo, J. Paek, and S. Bahk, "Deep-fading hole avoidance for secure region detection using channel state information," *J. Commun. Netw.*, vol. 24, no. 6, pp. 645–654, 2022.
- [15] I. Telatar and D. Tse, "Capacity and Mutual Information of Wideband Multipath Fading Channels," *IEEE Trans. Inform. Theory*, vol. 46, no. 4, pp. 1384–1400, 2000.
- [16] D. Puccinelli and M. Haenggi, "Multipath Fading in Wireless Sensor Networks: Measurements and Interpretation," in *Proc. IEEE IWCMC*, 2006.
- [17] A. Ghasemi and E. S. Sousa, "Fundamental Limits of Spectrum-Sharing in Fading Environments," *IEEE Trans. Wireless Commun.*, vol. 6, no. 2, pp. 649–658, 2007.
- [18] S. Tuelian, D. Bankov, D. Shmelkin, and E. Khorov, "IEEE 802.11ax OFDMA Resource Allocation with Frequency-Selective Fading," *Sensors*, vol. 21, no. 18, 2021.
- [19] Y. Son, S. Kim, S. Byeon, and S. Choi, "Symbol Timing Synchronization for Uplink Multi-User Transmission in IEEE 802.11ax WLAN," *IEEE Access*, vol. 6, pp. 72 962–72 977, 2018.
- [20] K. Wang and K. Psounis, "Scheduling and Resource Allocation in 802.11ax," in *Proc. IEEE INFOCOM*, 2018.
- [21] P. K. Sangdeh and H. Zeng, "DeepMux: Deep-Learning-Based Channel Sounding and Resource Allocation for IEEE 802.11ax," *IEEE J. Select. Areas Commun.*, vol. 39, no. 8, pp. 2333–2346, 2021.
- [22] Y. Son, K. Lee, S. Kim, J. Lee, S. Choi, and S. Bahk, "REFRAIN: Promoting Valid Transmission in High-Density Modern Wi-Fi Networks," in *Proc. ACM MobiHoc*, 2020.
- [23] H.-W. Lee and S. Chong, "Downlink resource allocation in multi-carrier systems: frequency-selective vs. equal power allocation," *IEEE Trans. Wireless Commun.*, vol. 7, no. 10, pp. 3738–3747, 2008.
- [24] C. Xiong, G. Y. Li, S. Zhang, Y. Chen, and S. Xu, "Energy-efficient resource allocation in ofdma networks," *IEEE Trans. Commun.*, vol. 60, no. 12, pp. 3767–3778, 2012.
- [25] Y. Son and S. Bahk, "Revisiting Wi-Fi Performance under the Impact of Corrupted Channel State Information," in *Proc. ACM MSWiM*, 2020.
- [26] D. Halperin, W. Hu, A. Sheth and D. Wetherall, "Predictable 802.11 Packet Delivery from Wireless Channel Measurements," in *Proc. ACM SIGCOMM*, 2010.
- [27] MathWorks, Physical Layer Abstraction for System-Level Simulation. [Online]. Available: <https://www.mathworks.com/help/wlan/ug/physical-layer-abstraction-for-system-level-simulation.html>.
- [28] K. Brueninghaus, D. Astely, T. Salzer, S. Visuri, A. Alexiou, S. Karger, and G-A. Seraji, "Link Performance Models for System-Level Simulations of Broadband Radio Access Systems," in *Proc. IEEE PIMRC*, 2005.
- [29] F. Bourgeois and J.-C. Lassalle, "An extension of the munkres algorithm for the assignment problem to rectangular matrices," *Commun. ACM*, vol. 14, no. 12, pp. 802–804, 1971.
- [30] Z. Jiang, T. H. Luan, X. Ren, D. Lv, H. Hao, J. Wang, K. Zhao, W. Xi, Y. Xu, and R. Li, "Eliminating the Barriers: Demystifying Wi-Fi Baseband Design and Introducing the PicoScenes Wi-Fi Sensing Platform," *IEEE Internet Things J.*, vol. 9, no. 6, pp. 4476–4496, 2021.
- [31] MathWorks, MATLAB R2024a, WLAN System Toolbox. [Online]. Available: <https://www.mathworks.com/help/wlan/>.
- [32] IEEE P802.11, *TGax Channel Models*, Sep. 2014.
- [33] Network Simulator ns-3. [Online]. Available: <http://www.nsnam.org/>.
- [34] K. Lee, J. Shin, J. Park, Y. Son, and S. Bahk, "Recovering CSI and Data in Dense Network Environments using IEEE 802.11ax Midamble," *IEEE Access*, vol. 11, pp. 65 858–65 871, 2023.
- [35] MadWiFi, Minstrel rate control. [Online]. Available: [http://madwifi-project.org/browser/madwifi/trunk/ath\\_rate/minstrel](http://madwifi-project.org/browser/madwifi/trunk/ath_rate/minstrel).